Ground state and the metal-insulator transition in $(Pr_{1-y}Y_y)_{1-x}Ca_xCoO_3$ (0.45≤x≤0.55) cobaltites

A. J. Barón- González[1], J. L. García- Muñoz[1], J. Herrero- Martín[1], C. Frontera[1], G. Subías[2] and J. Blasco[2]

[1]*Institut de Ciència de Materials de Barcelona, ICMAB-CSIC, Campus Univ. de Bellaterra, E-08193 Bellaterra, Spain*

[2]*Instituto de Ciencias de Materiales de Aragón, CSIC-Universidad de Zaragoza, c/ Pedro Cerbuna 12, 50009 Zaragoza, Spain*

Abstract

$Pr_{0.5}Ca_{0.5}CoO_3$ exhibits a non-conventional metal-insulator transition (MIT) in which the insulating state is due to a volume contraction (~2%) and electron transfer from Pr to Co sites. $Pr_{1-x}Ca_xCoO_3$ cobaltites with Ca doping around x~0.5 (0.45≤x≤0.55) have been investigated. Different ground states and phase transitions are reported in samples at both sides of the half-doped composition. The relevance of the Pr/Ca ratio around half-doping and the amplitude of the changes observed at the MIT are analyzed. Besides the expected variation in the transition temperature, we report an enhanced Pr^{3+}/Pr^{4+} transformation at the MIT in $Pr_{0.45}Y_{0.05}Ca_{0.50}CoO_3$ [0.25(5) e^-/ Pr ion and T_{MI}=120 K] with respect to $Pr_{0.5}Ca_{0.5}CoO_3$ [0.15(5) e^-/ Pr ion and T_{MI}=75 K].

I. INTRODUCTION

Metal-insulator transitions (MIT) in cobaltites are attracting great interest due to the relevance of the spin state of Co for electron mobility in these strongly correlated oxides .[1-7] Rich properties of cobaltites containing trivalent cobalt are linked to the comparable energies of its crystal field and intra-atomic electron-electron coupling. $Pr_{0.5}Ca_{0.5}CoO_3$ exhibits a MIT and it is considered a strongly correlated spincrossover system. [6] The carriers introduced by doping in $Pr_{1-x}Ca_xCoO_3$ can be viewed as low spin (LS) Co^{4+} (S=1/2, t^5_{2g}) species moving through the matrix of intermediate spin (IS) Co^{3+} (S=1, $t^5_{2g}e_g^1$) centers. Initially the MIT (T_{MI}≈75 K.) in $Pr_{0.5}Ca_{0.5}CoO_3$ was attributed to a sudden change of IS Co^{3+} ions to its LS state (S=0, $t^5_{2g}e_g^0$) [6]. The generation of metallic domains in the insulating low temperature phase of $Pr_{0.5}Ca_{0.5}CoO_3$ by ultrafast photoexcitation was reported in ref. 8.

At low doping levels (x<0.2) $Pr_{1-x}Ca_xCoO_3$ samples are insulating, without long-range magnetic ordering.[9] Increasing doping beyond x=0.2 the oxides are metallic and exhibit long-range ferromagnetic (FM) order below 60-70K. Increasing the Ca content induces a more homogeneous magnetism. It has been claimed that short-range FM order coexists with long-range ferromagnetism at moderate dopings. [10] Around half doping a MIT may develop at relatively low temperature (T_{MI}~75 K for x=0.50). In the insulating state $Pr_{0.5}Ca_{0.5}CoO_3$ shows no evidence of spontaneous long-range magnetic order.

In addition, the first order MIT is only found as a function of temperature or applied pressure in $(Pr_{1-y}Ln_y)_{1-x}Ca_xCoO_3$ compositions having Pr atoms.[11] Both *x* and *y* parameters and the lanthanide species have a strong influence on the MIT. It is generally assumed that

main effect of small lanthanides like yttrium is moving the transition towards higher temperatures due to the enhancement of the orthorhombic distortion [11].

Recent findings demonstrate an active participation of the 4f electrons of Pr [12-15] and a rather singular mechanism for this MIT. A significant volume reduction of ~2% in $Pr_{0.5}Ca_{0.5}CoO_3$ across T_{MI} is the result of an exceptional Pr-O bond shortening in the insulating state.[16,17] X- ray absorption experiments (XAS) on $Pr_{0.5}Ca_{0.5}CoO_3$ have evidenced a Pr^{3+}/Pr^{4+} valence transition at T_{MI}.[14,15] Electrons leaving Pr sites are used to stabilize the trivalent low-spin state of Co[12-15]. Present work focuses on a narrow range of Ca and Y doping in $(Pr_{1-y}Y_y)_{1-x}Ca_xCoO_3$ around the reference cobaltite $Pr_{0.5}Ca_{0.5}CoO_3$.

II. EXPERIMENTAL

$Pr_{1-x}Ca_xCoO_3$ (x=0.45, 0.50 and 0.55) and $Pr_{0.45}Y_{0.05}Ca_{0.50}CoO_3$ were prepared in polycrystalline form by solid-state reaction as detailed elsewhere[17]. To reach the optimal oxygen content ($O_{3-\delta}$ with δ=0) the samples were finally treated under high oxygen pressure (at 900ºC with P_{O2}=200 bar during 14 hours, and at 475ºC with P_{O2}=150 bar during 6 hours). Samples were fully stoichiometric according to Rietveld analysis of neutron diffraction (NPD) data. NPD patterns were collected on D2B [λ=1.594 Å], D1B [λ=2.52 Å] and D20 [λ=1.88 Å] diffractometers of ILL (Grenoble), in the temperature range between 5 K and room temperature (RT). Magnetization and transport measurements were performed using a superconducting quantum interference device (SQUID) magnetometer and commercial Physical Properties Measurement System (PPMS). X-ray absorption spectra were recorded in beamline PM3 at the synchrotron radiation source of the Helmholtz Zentrum in Berlin by the total electron yield detection mode, with an energy resolution better than 0.3 eV at 900 eV. Hereafter we will refer to

$Pr_{0.55}Ca_{0.45}CoO_3$, $Pr_{0.50}Ca_{0.50}CoO_3$, $Pr_{0.45}Ca_{0.55}CoO_3$ and $Pr_{0.45}Y_{0.05}Ca_{0.50}CoO_3$ as PCCO45, PCCO50, PCCO55 and PYCCO respectively.

III. RESULTS

The resistivity and magnetization of the $Pr_{1-x}Ca_xCoO_3$ samples with doping below (x=0.45) and above (x=0.55) the half-doped composition are plotted in Fig. 1, where they are compared to PCCO50. This figure provides the first evidence of a different behaviour for $x \leq 0.50$ and $x \geq 0.50$. The temperature dependence of the resistivity (ρ) in PCCO55 shows a sudden change in the conductivity of one order of magnitude below T_{MI}~70K. This critical temperature is very similar to that measured in the half-doped perovskite (~75K), where the change in the conductivity is 10 times larger.[6,14] The drop in the susceptibility is a characteristic feature of the transition in PCCO50. It could be mainly attributed to the entering of the Co^{3+} LS state, which must also be responsible for the absence of long-range magnetic order in the insulating state. A similar evolution of the susceptibility is seen in PCCO55, although the susceptibility drop in this case is smaller than in PCCO50. There is no sign of ferromagnetic order in any of these two compositions below T_{MI}. This contrasts with the onset of ferromagnetism in PCCO45 below T_C~80K [Fig. 1(b)]. At 2 K the zero-field magnetization extrapolated from $M(H)$ yields a ferromagnetic moment $M_0 = 0.55 \mu_B$ /f.u. Moreover, the resistivity of PCCO45 displays a metallic behaviour (of "bad metal" type) in the whole T-range down to 2 K. So, PCCO45 is a ferromagnetic metal below Tc. In addition there is a gain of conductivity in the ferromagnetic phase, as is typically observed in other double-exchange metallic cobaltites.

In Fig. 2(a) we plot the thermal evolution of (112)/(031) and (220)/(131) reflections obtained from medium-resolution NPD in PCCO55. A marked and sudden shift in the

angular position of the diffraction lines towards higher 2θ angles can be observed on cooling around 70K. A volume contraction cooling the slightly overdoped compound shifts the diffracted reflections towards higher *Q*-values. This has not been observed in PCCO45, the slightly underdoped compound. Quantitatively, the temperature dependence of the unit cell volume in these two compounds was obtained from the analysis of diffraction patterns collected at fixed selected temperatures.

The evolution of the cell parameters in PCCO45, and PCCO55 is shown in Fig. 3. The absence of structural anomalies is apparent in the former [Fig. 3(a)]. In PCCO55 the anisotropic changes in the cell dimensions mimic the changes reported in half-doped PCCO50.[16,17] Although, as we pointed out comparing the resistivities of PCCO50 and PCCO55, the amplitude of the structural changes in PCCO55 are slightly smaller than in PCCO50.

In $Pr_{0.45}Y_{0.05}Ca_{50}CoO_3$ (PYCCO) Ytrium partially substitutes Praseodimium while keeping the ratio $Co^{4+}/ Co^{3+}=1$. The evolution of its resistivity plotted in Fig. 4 shows a MIT around 120 K, a temperature ~45 K higher than the transition in PCCO50. In the inset of Fig. 4 we have reproduced the evolution of the volume corresponding to PCCO50 [14,17], and have also plotted the contraction of the volume in PYCCO obtained from neutron data.

In figure 5 we show the X- ray absorption spectra of PYCCO at the Pr $M_{4,5}$ edges ($3d \rightarrow 4f$ electronic transitions) at different T values. There are evident spectral changes at both edges, the main evolution taking place at $T \sim T_{MI}=120$ K. The enhancement of the absorption signal in the ~ 934-941 eV and ~ 952-960 eV energy intervals at $T<T_{MI}$ reflects the appearance of a certain quantity of Pr^{4+} ions in the low *T* insulating phase[15]. A quantification of the electronic charge transferred from Pr to Co ions can be done by the

weighted addition method of selected references, as shown in the inset of Fig. 5. The method is explained in detail in ref. 15, where we applied it to PCCO50. From a similar study of the Pr $M_{4,5}$ edges across the transition in PCCO50 we concluded that 0.15(5) e^- are transferred from (in average) each Pr ion to Co sites at 10 K as compared to their electron occupancy at 300 K. For PYCCO, the same analysis method yields 0.25(5) e^-/ Pr ion at 20 K as compared to 300 K.

IV. DISCUSSION AND CONCLUSIONS

We have shown an asymmetry in the ground state of $Pr_{1-x}Ca_xCoO_3$ cobaltites around x=0.50. With a slightly lower Ca content (x=0.45) the system is metallic at low temperature, whereas it is insulating for slightly higher dopings (x=0.55). In this study all the samples were oxygenated using high oxygen pressure. This is essential for compositions with $x \geq 0.50$ because the difficulties to obtain fully oxygenated samples increase with Ca content. From present results we can conclude that the largest change of conductivity at the MIT in $Pr_{1-x}Ca_xCoO_3$ samples must occur within the $0.45<x<0.55$ interval.

We mainly attribute the qualitatively different behaviour observed in PCCO45 and PCCO55 to a subtle but effective change in the orthorhombic *Pnma* (of $GdFeO_3$-type) distortion caused by a reduction from 0.55 to 0.45 in the Ca content. Despite both ionic sizes are very similar, Pr^{3+} is slightly larger than Ca^{2+} (1.126 and 1.120 Å in radius, respectively[18]) thus decreasing the tilting of CoO_6 octahedra in PCCO45 with respect to PCCO55. We have confirmed this point by a Rietveld analysis of our NPD data. The overall $GdFeO_3$-type distortion at RT (represented by the $\langle\theta\rangle=\langle$Co-O-Co$\rangle$ bond angle) in PCCO45, PCCO50, PCCO55 and PYCCO is $\langle\theta\rangle$=158.17(3)°, 158.03(6)°, 157.94(8)° and 157.49º, respectively. The effect associated to the Pr content is thus double: (*i*) on one

hand its presence makes possible a strong Pr(4*f*)-O(2*p*) hybridization (origin of the anomalous volume reduction). (*ii*) On the other, an excess of Pr atoms inhibits the anomalous Pr-O hybridization and Pr^{3+}/ Pr^{4+} valence shift. The reason for the latter is that it reduces the tilting of CoO_6 octahedra moving away the apical oxygens from the positions occupied by Pr atoms. This hampers the Pr(4*f*)-O(2*p*) hybridization and explains the absence of an anomalous contraction of the cell at low temperature in PCCO45 (ferromagnetic metal). It also explains the behaviour of PYCCO as shown in the inset of Fig. 4. Finally, the tilting of the octahedra in PCCO55 is larger than in PCCO50. The <Co-O-Co)> bonding angle decreases thus favouring the Pr(4*f*)-O(2*p*) hybridization. However, the lower Pr content reduces the density of Pr^{4+}-O bonds below the transition. This justifies that the changes observed in PCCO55 across the MIT (Figs. 1, 2) are more modest than in PCCO50. Hence, these results can be well understood within the valence change model and suggest a strongly inhomogeneous behaviour at higher doping levels (x>0.55).

Finally, we can extract additional conclusions from our comparative analysis of the behaviour of half-doped $Pr_{0.45}Y_{0.05}Ca_{50}CoO_3$ (PYCCO) and $Pr_{0.5}Ca_{0.5}CoO_3$ (PCCO50) compounds. From NPD data at RT we have obtained the <Co-O-Co)> distortion angles <θ>=157.49(8)° and 158.03(6)° for PYCCO and PCCO50. Besides the expected enhancement of the transition temperature in the former, the analysis of the XAS spectra at the Pr $M_{4,5}$ edges of PYCCO allows us to conclude about the intensity of the Pr^{3+}/Pr^{4+} transformation at the transition. We have observed an enhanced Pr^{3+}/Pr^{4+} transformation in PYCCO (0.25(5) e^-/ Pr ion) with respect to PCCO50 (0.15(5) e^-/ Pr ion [15]). To be noted is that these are estimations per Praseodymium atom, and therefore do not refer to the overall charge transfer from Pr to Co sites per formula unit.

ACKNOWLEDGMENTS

We thank financial support from MICINN (Spanish government) under projects No. MAT2009-09308 and No. CSD2007-00041 (NANOSELECT) and CRG-D1Band the ILL and HZB for granting beamtime. J.H.-M. thanks CSIC for JAEDoc contract, cofinanced by the European Social Fund. We also thank R. Abrudan and S. Valencia for technical support..

References

[1] I. O. Troyanchuk, N. V. Kasper, D. D. Khalyavin, H. Szymczak, R. Szymczak, and M. Baran, Phys. Rev. Lett. **80**, 3380, (1998).

[2] J.B. Goodenough, J. Phys. Chem. Solids **6**, 287 (1958).

[3] M.A. Señarís-Rodríguez and J.B. Goodenough, J. Solid State Chem. **116**, 224 (1995).

[4] T. Saitoh, T. Mizokawa, A. Fujimori, M. Abbate, Y. Takeda, and M. Takano, Phys. Rev. B **55**, 4257 (1997).

[5] C. Frontera, J.L. García-Muñoz, A. Llobet and M.A.G. Aranda, Phys. Rev. B **65**, 180405(R) (2002).

[6] S. Tsubouchi, T. Kyômen, M. Itoh, P. Ganguly, M. Oguni, Y. Shimojo, Y. Morii, and Y. Ishii, Phys. Rev. B **66**, 052418 (2002).

[7] A. Maignan, V. Caignaert, B. Raveau, D. Khomskii and G. Sawatzky, Phys. Rev. Lett. **93**, 026401 (2004).

[8] Y. Okimoto, X. Peng, M. Tamura, T. Morita, K. Onda, T. Ishikawa, S. Koshihara, N. Todoroki, T. Kyomen, and M. Itoh, Phys. Rev. Lett. **103**, 027402 (2009).

[9] S. Tsubouchi, T. Kyômen, M. Itoh and M. Oguni, Phys. Rev. B **69**, 144406 (2004).

[10] S. El-Khatib, S. Bose, C. He, J. Kuplic *et al*, Phys. Rev. B **82**, 100411R (2010).

[11] T. Fujita, S. Kawabata, M. Sato, N. Kurita, M. Hedo, and Y. Uwatoko, J. Phys. Soc. Jpn. **74**, 2294 (2005).

[12] K. Knížek, J. Hejtmánek, P. Novák, and Z. Jirák, Phys. Rev. B **81**, 155113 (2010).

[13] J. Hejtmánek, E. Šantavá, K. Knížek, M. Maryško, Z. Jirák, T. Naito, H. Sasaki, and H. Fujishiro, Phys. Rev. B **82**, 165107 (2010).

[14] J.L. García-Muñoz, C. Frontera, A.J. Barón-González, S. Valencia, J. Blasco, R. Feyerherm, E. Dudzik, R. Abrudan and F. Radu, Phys. Rev. B **84**, 045104 (2011)

[15] J. Herrero- Martin, J. L. García- Muñoz, S. Valencia, C. Frontera, J. Blasco, A. J. Baron-González, G. Subias, R. Abrudan, F. Radu, E. Dudzik, and R. Feyerherm, Phys. Rev. B **84**, 115131 (2011).

[16] A. Chichev, J. Hejtmánek, Z. Jirák, K. Knížek, M. Maryško, M. Dlouhá, and S. Vratislav, J. Magn. Magn. Mater. **316**, e728 (2007).

[17] A. J. Barón-González, C. Frontera, J. L. García-Muñoz, J. Blasco, and C. Ritter, Phys. Rev. B **81**, 054427 (2010).

[18] R. D. Shannon, Acta Cryst. Sect. A **32**, 751 (1976).

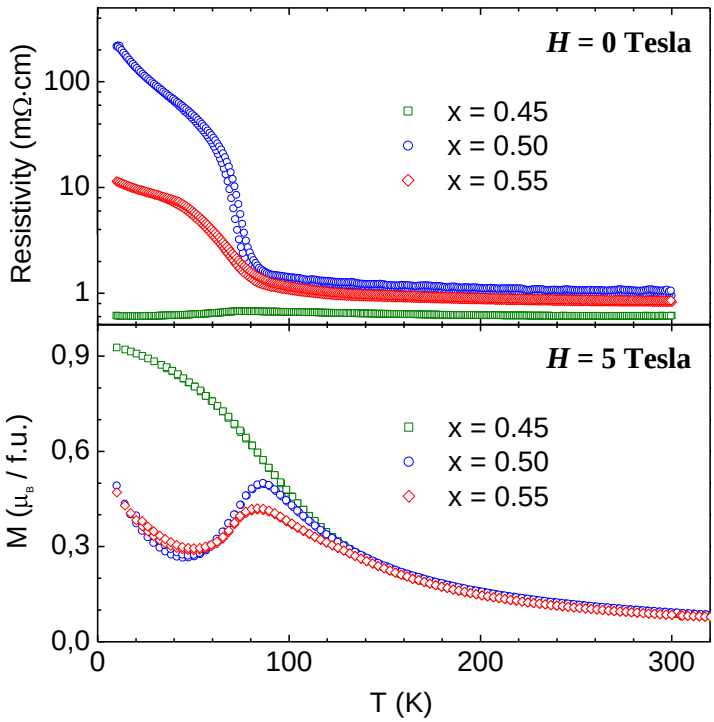

Figure 1. (a) Electrical resistivity of $Pr_{0.55}Ca_{0.45}CoO_3$, $Pr_{0.50}Ca_{0.50}CoO_3$ and $Pr_{0.45}Ca_{0.55}CoO_3$. (b) Magnetic susceptibility of the same samples as measured at 5 Tesla applied field.

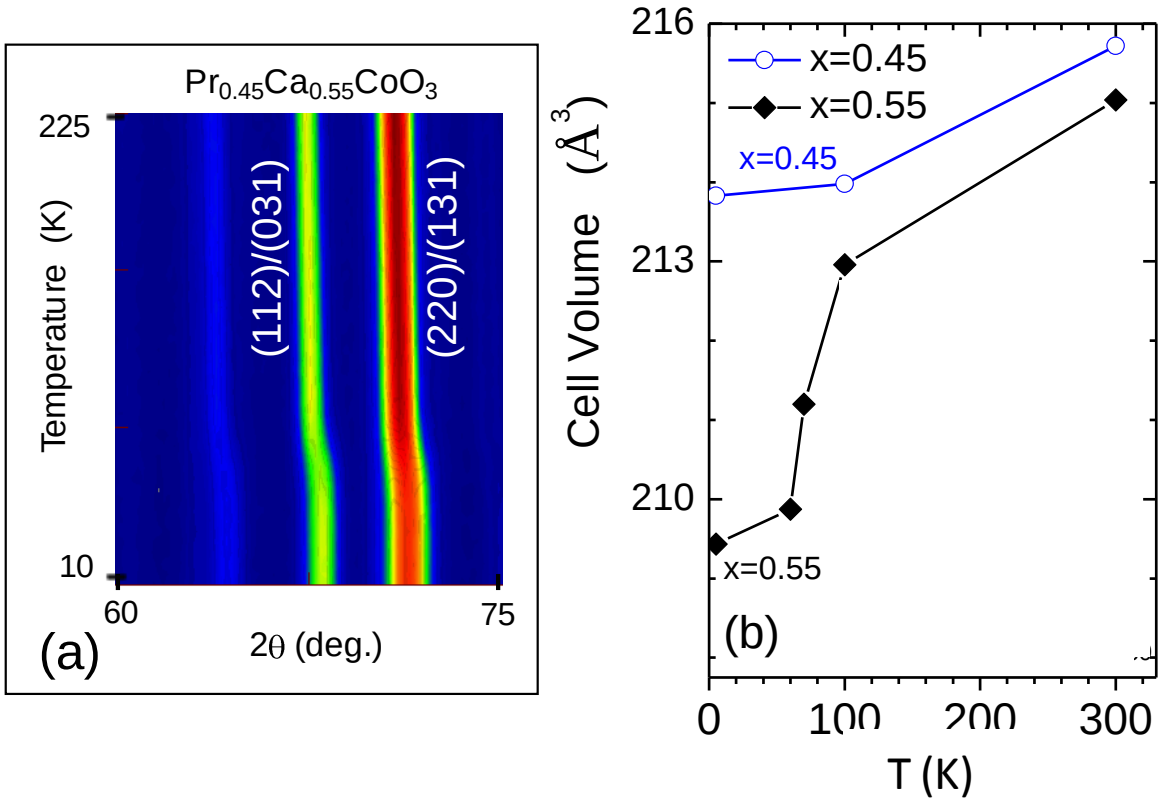

Figure 2. (a) Neutron diffracted intensities for (112)/(031) and (220)/(131) reflections in $Pr_{0.45}Ca_{0.55}CoO_3$ as a function of T (θ-2θ projection). (b) Thermal evolution of the crystal unit cell volume in $Pr_{1-x}Ca_xCoO_3$ cobaltites with x=0.45 and 0.55

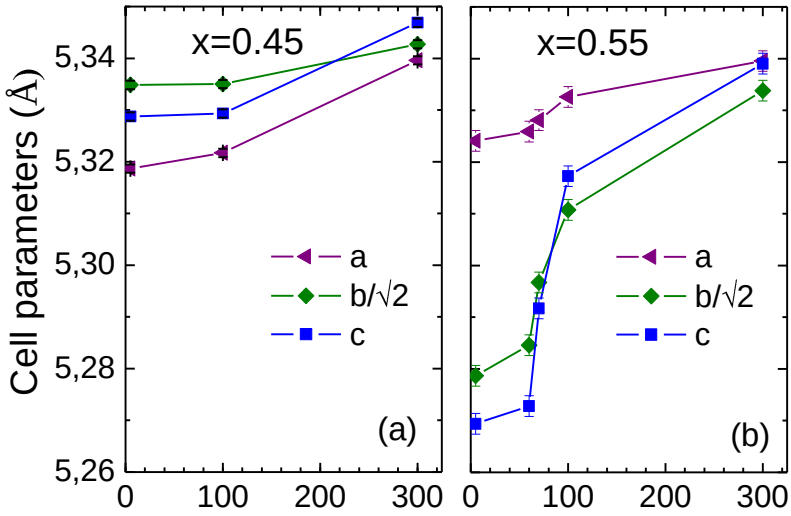

Figure 3. (a) Thermal evolution of the crystallographic lattice parameters in $Pr_{1-x}Ca_xCoO_3$ with Ca content (a) below (x=0.45) and (b) above (x=0.55) the half-doping composition.

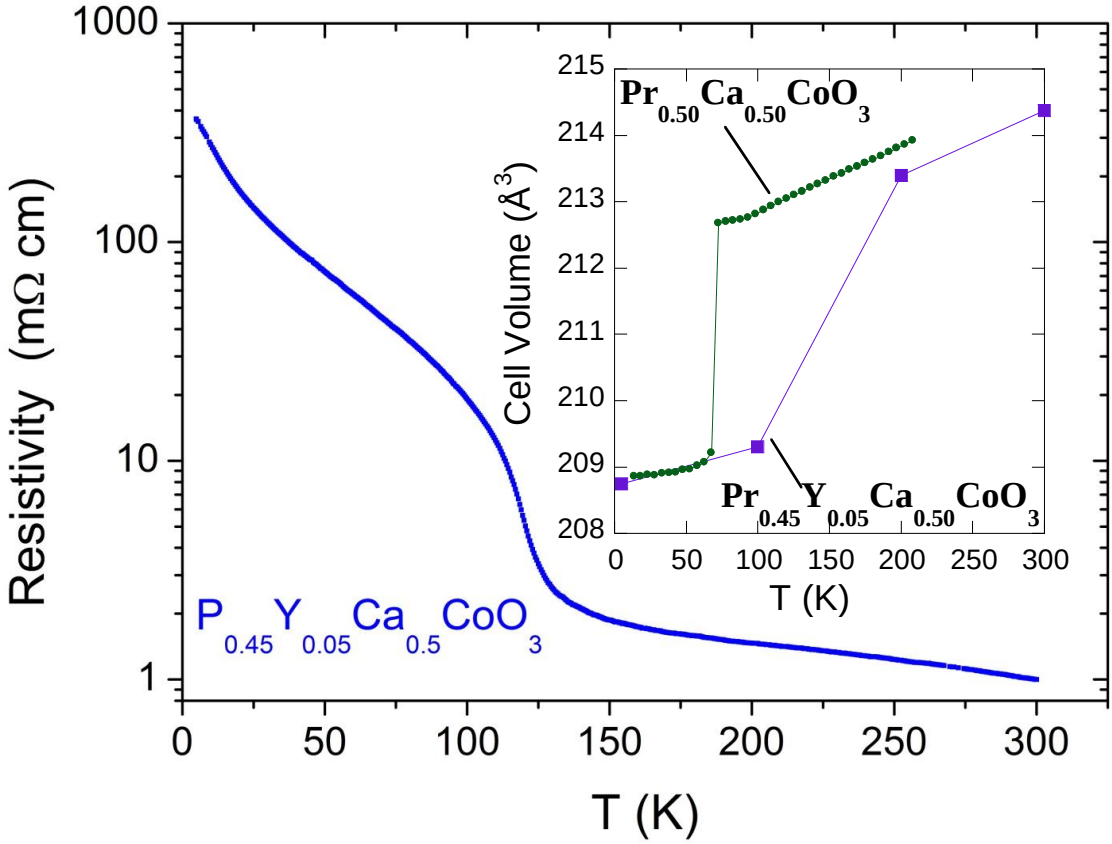

Figure 4. Electrical resistivity of PYCCO (blue dots) as a function of temperature, from 5 to 300 K illustrating the MIT at T_{MI}= 120 K. The inset shows the cell volume evolution of PYCCO (violet squares) in the corresponding thermal range as compared to that of PCCO50 (green circles).

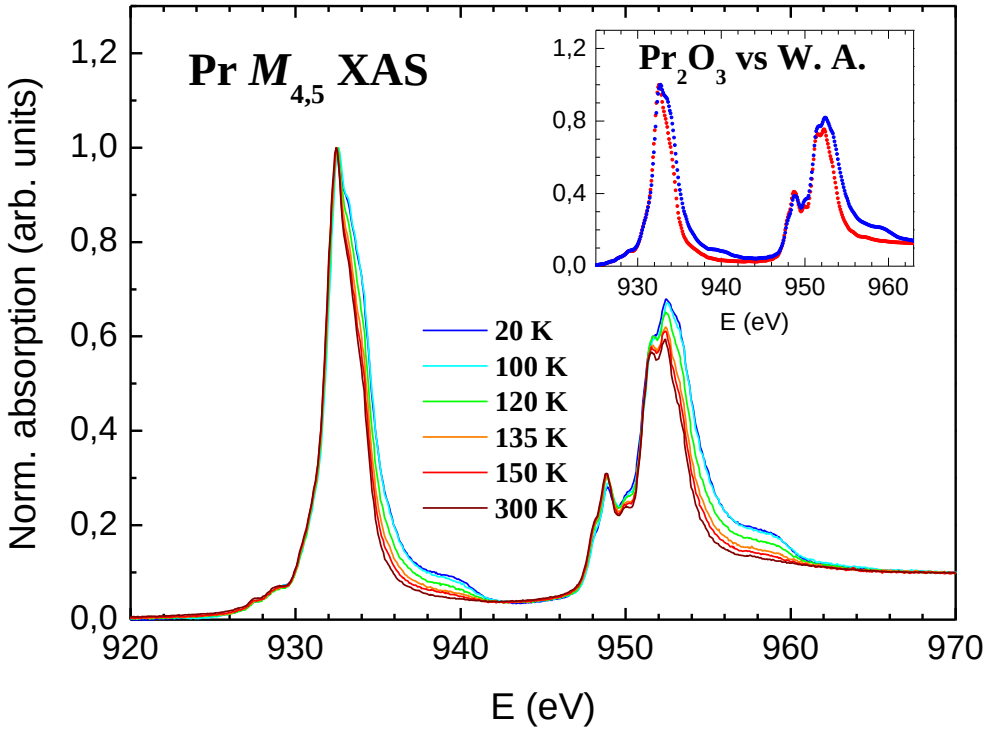

Figure 5. X- ray absorption spectra of $Pr_{0.45}Y_{0.05}Ca_{0.50}CoO_3$ (PYCCO) at the Pr $M_{4,5}$ edges as a function of temperature. The inset shows the weighted addition (W. A.) of the absorption spectra of Pr_2O_3 (Pr^{3+}) and $BaPrO_3$ (Pr^{4+}) in a 1:0 (red circles) and 3:1 (blue circles) ratio, which helps to estimate the Pr→Co charge transfer in PYCCO across the MIT.